The Savage-Hutter Avalanche Model How far Can it be Pushed?

Kolumban Hutter, Yongqi Wang and Shiva P. Pudasaini
Department of Mechanics
Darmstadt University of Technology
64289 Darmstadt, Germany
{hutter,wang,pudasain}@mechanik.tu-darmstadt.de

Abstract

The Savage-Hutter (SH) avalanche model is a depth averaged dynamical model of a fluid like continuum implementing the following simplifying assumptions: (i) density preserving, (ii) shallowness of the avalanche piles and small topographic curvatures, (iii) Coulomb-type sliding with bed friction angle δ and (iv) Mohr-Coulomb behaviour in the interior with internal angle of friction $\phi \geq \delta$ and an ad-hoc assumption reducing the number of Mohr's circles in three dimensional stress states to one. We scrutinize the available literature on information regarding these assumptions and thus delineate the ranges of validity of the proposed model equations. The discussion is limited to relatively large snow avalanches with negligible powder snow component and laboratory sand avalanches starting on steep slopes. The conclusion of the analysis is that the SH model is a valid model for sand avalanches, but its Mohr–Coulomb sliding law may have to be complemented for snow avalanches by a second viscous contribution. For very small snow avalanches and for laboratory avalanches starting on moderately steep and bumpy slopes it may not be adequate.

1 Introduction

The Savage-Hutter (SH) avalanche model [34, 35] and its extensions [5, 7, 8, 12, 13, 14, 15, 16, 21, 28, 29, 38, 40, 44], henceforth also called SH-model, is a dynamical fluid-like model which consists of hyperbolic partial differential equations for the distribution of the depth and the (two) topography-parallel, depth averaged velocity components in an avalanching mass of cohesionless granules (e.g., sand, grains, rocks and snow). It is designed to predict the motion and deformation from initiation to runout along a concomitantly determined avalanche track along a prescribed topography. In the past, it has been used to describe flows in straight and curved chutes [7, 13, 14, 15, 16], in channels with plane and parabolic cross sections and simply curved thalwegs [5, 8, 11, 21, 22, 38, 39, 41, 42], but has been extended to flows in corries having arbitrarily curved and twisted thalwegs and arbitrary topographies [28, 29, 30]. The basic simplifying assumptions in the various models are mathematically not exactly the same; however, physically they are identical, namely consisting of

(i) the assumption of density preserving (incompressibility),

(ii) the assumption of shallowness of the avalanche piles, and of small topographic curvatures,

(iii) the assumptions of Coulomb-type sliding with bed friction angle δ,

(iv) Mohr–Coulomb frictional behaviour in the interior with internal angle of friction $\phi \geq \delta$ and an ad-hoc assumption, reducing the number of Mohr's circles in three dimensional stress states from three to one, and

(v) nearly uniform velocity profile through the avalanche depth.

All these assumptions can be justified, but they limit the applicability of the model equations. In the ensuing study we scrutinize the literature and provide documentation under what conditions the SH-avalanche equations are likely to be valid. Specifically, it is shown both for laboratory avalanches and for flow avalanches of snow that the above stated five simplifying assumptions are not invalidating the model equations to the extent that they would not be able to reproduce laboratory and field experiments sufficiently accurately. This is not to say that one or the other assumption (i)–(v) would always be fulfilled, but that its violation may be minor or, if it is large, of short duration or length as compared to the global scales, that it will hardly be identifiable in laboratory or large scale observations. This neither means that there would not be a number of situations in which the model equations fail as an adequate predictive tool. This happens for instance for very small snow avalanches (slab avalanches) or for avalanches starting on slopes with small inclination angle, for slush avalanches or for the motion over very rough beds or abrupt topographic steps. All these cases are mainly short-lived and thus do not reach a catastrophic level.

In §2 the ranges of validity of the aforementioned five assumptions will be identified; it deals with laboratory experiments and field observations, and the assumptions (i)–(v) will be justified. The performance of the model equations will be discussed in §3; this means that model output will be compared with the corresponding findings from experiments, but it equally also relates to the computational performance of numerical codes in attempts to integrate the free boundary value equations. Finally, §4 brings an outlook of unsolved problems to be handled in the future.

2 The simplifying assumptions and their ranges of validity

2.1 Density preserving

There are hardly any measurements available on volume changes in rapid shear flows of snow or granular materials. However, Hutter & Koch [13] reported measurements of areal changes of granular flows in an exponentially curved chute of 10 cm width by taking fast speed photographs from the side and measuring the areas of the individual pile shapes. These measurements revealed volume changes in sand-avalanche-chute flows initially of 15–20%, i.e., between the pile volume at rest and that of the first photograph in motion, less than $\sim 4\%$ during motion, i.e., between any two photographs when the

avalanche was moving and inconclusive information during the settling process. This is consistent with what one would expect: A considerable expansion when the granular mass is set into shearing, practically remaining density preserving in rapid flow and experiencing a compaction when the avalanche stops suddenly or continuously.

Field observations on density variations in artificially released flow avalanches of snow were made by Gubler and others [9, 10]. These authors use microwave FMCW techniques. Their measurements provide limited information about the density variation with depth of the snow in motion, but the results are not conclusive enough to infer that density variations would play a dynamic role in the avalanche motion.

Qualitatively, these results are plausible. Snow avalanches in the flowing regime are relatively dense, bouncing is seldom seen, much less than in laboratory sand flows, and when so, only in dry snow avalanches. So, the mean particle distances are likely not much larger than the particle diameters. Moreover, shearing seems to be weak and restricted to the thin fluidized layer at the base, which is most likely small (see also velocity measurements later on). So, the depth changes due to the associated dilatations are small. It follows that the conditions of a Boussinesq medium are satisfied, but since no traces of buoyancy effects have been seen *the assumption of density preserving is an excellent approximation.*

2.2 Shallowness of the avalanche piles – small topographic curvature

Observations of dense flow avalanches show that the moving snow masses are thin, long and wide and have an aspect ratio

$$\varepsilon = \frac{\text{typical thickness } [H]}{\text{typical length tangential to the bed } [L]} \ll 1,$$

which is very small and is of order $10^{-3} - 10^{-1}$. Avalanches with large aspect ratios ($\varepsilon \sim 1$) are generally small, travel short distances and practically never cause damage nor constitute a danger. Therefore, they are less important. So, approximating non-dimensionalized equations to terms linear in ε may be sufficient. This also requires that local radii $[R]$ of the topography are large such that $[L]/[R] = \mathcal{O}(\varepsilon^\alpha)$, $0 < \alpha < 1$, that the coefficient of bed friction angle is equally $\mathcal{O}(\varepsilon^\beta)$, $0 < \beta < 1$, and that dimensionless shearing in the bulk velocity profile is $\mathcal{O}(\varepsilon^{1+\gamma})$, with $\gamma = \min\{\alpha, \beta\}$. These assumptions are stringent restrictions. Topographic variations must be relatively smooth, basal friction ought to be limited (namely $\delta \leq \phi$), so bumpy bottom boundaries are excluded. Moreover, in reality topographic regions with large curvature are often small and then may only have a limited effect on the overall flow of the avalanche. When, on the other hand, avalanches chute over a topographic step and become air borne and go through a ballistic motion, they often turn into a powder snow avalanche after impinging on the ground. In these situations the model, of course, ceases to be valid. On the other hand, todays Geographical Information Systems (GIS) are usually based on a $25 \times 25\,\mathrm{m}^2$ grid, whilst a $5 \times 5\,\mathrm{m}^2$ grid would be more appropriate; therefore they do not allow to resolve the topography sufficiently accurately to account for local bumps and troughs.

Thus, the shallowness assumption is reasonably satisfied and may only occasionally be violated. In circumstances when it is only locally violated the simplified model

equations are likely to generate reasonable solutions, see [14].

2.3 Bed friction only Coulomb-type

All classical avalanche models write the basal shear stress as a combination of a normal-stress dependent Coulomb term and a velocity dependent viscous terms

$$\text{Basal shear} = \text{Coulomb term} + \text{Viscous contribution},$$
$$\boldsymbol{\tau}_{\text{Base}} = -\left\{(\tan\delta)p_\perp \frac{\boldsymbol{v}}{|\boldsymbol{v}|} + c(\boldsymbol{v}, p_\perp)|\boldsymbol{v}|\boldsymbol{v}\right\},$$

in which δ is the bed-friction angle, $p_\perp$ the pressure normal to the base, c the viscous drag coefficient, generally treated as constants but varying from avalanche to avalanche, and $\boldsymbol{v}$ is the velocity tangential to the bed, see Voellmy [42], Perla et al. [26], Salm et al. [31, 32]. Hutter and others almost exclusively set $c = 0$ and state that granular avalanches in the laboratory can be well reproduced by the Coulomb term alone [5, 7, 8, 9, 11, 12, 13, 14, 15, 16], sometimes by accounting for a reduction in the value of δ in the rear portion of the avalanche, [5, 45], because abraded and deposited fines reduce the bed friction angle. On the other hand, identifications of δ and c from observations and back calculation of field avalanches, come up with both, nonzero δ and c, see e.g. Ancey [1, 2], Gubler et al. [9], Gubler [10], Zwinger and others [46, 47]. For the runout process shortly before the avalanche comes to an immediate stop, there were even suggestions to parameterize c as $c \propto |\boldsymbol{v}|^{-3}$, see Schaerer [36].

It is well known that with a Coulomb sliding law alone and a constant bed friction angle, a steady flow[1] of an avalanche down an inclined plane cannot be obtained; the avalanche is continuously accelerating. (See, however, the work of Savage & Nohguchi [33] for an exponentially curved bed and when δ is not a constant; and work by Hutter [11], Hutter & Greve [12], Hutter & Nohguchi [15]). Based on this, it is sometimes argued that, if the steady state motion exists, an additional friction process, e.g. a viscous component is needed. In the field, this question can probably never be settled. Verification is not possible, since avalanche tracks are not plane, not uniformly rough and generally too short in the sense of producing steady state behaviour. At least as far as field avalanches are concerned, an additional friction mechanism only needs to be added, when large discrepancies with observations arise. From this it follows that existence of a steady asymptotic flow in natural events is rather a belief of the scientist demanding it than an established fact. Careful experiments done with granular avalanches along plexiglass chutes show no conclusive information as to whether steady state flows will asymptotically be reached[2], see Eckart et al. [4].

In a recent paper, in which Ancey and Meunier [2] performed a back analysis of 15 documented avalanche events, the bulk frictional force, experienced by an avalanche was computed. "Three types of rheological behaviour were identified: (i) the inertial regime, where the frictional force drops to zero, (ii) the Coulombic frictional force, where the force is fairly independent of the avalanche velocity, and (iii) the velocity-dependent regime, where the force exhibits a complicated (nonlinear and hysteretic) dependence on velocity. During its course, an avalanche can experience one or several regimes.

[1] The centre of mass of a finite mass is moving steadily; the avalanche can still deform.

[2] In these experiments δ and ϕ were similar to those also relevant in dense flow avalanches

Interestingly, the Coulomb model can provide predictions of the velocity and runout distance in good agreement with field data for most events, even though for some path sections, the bulk frictional force departs from the Coulomb model", from [2].

Results obtained by Zwinger [46] point in a slightly different direction. He models mixed avalanches consisting of powder and flow avalanche components, in which the SH-flow avalanche component is used in combination with a turbulent, particle laden powder avalanche with a coupling through a saltation layer. In post computations of the Madlein avalanche of 1984 in the community Ischgl he found that reasonable agreement with the observed deposition could only be obtained when the sliding law was Coulomb-type at low velocities and viscous-type at large velocities. No extensive parameter study seems to have been made by Zwinger, so that better agreement would also be possible when a careful parameter identification would be made. Besides this, the Madlein avalanche is mixed and thus of a different class.

All these findings converge to the statement that Coulomb friction only needs to be complemented by a viscous drag under unusual circumstances.

2.4 Shearing is unimportant except at the very base

Typical internal, ϕ, and bed, δ, friction angles for real snow avalanches and for laboratory avalanches of quartz, sand, marmor chips and vestolen (plastic beads) moving on plexiglass chutes or chutes coated with drawing paper and sandpaper (SIA120), respectively, are

$$\begin{aligned} \text{Snow:} \quad & 30^\circ < \phi < 40^\circ, \quad 13^\circ < \delta < 22^\circ, \\ \text{Lab sand:} \quad & 30^\circ < \phi < 37^\circ, \quad 19^\circ < \delta < 25^\circ. \end{aligned}$$

This guarantees that the basal surfaces are smoother than the material under motion, and the absence of the bumpiness makes it unlikely that the bed transmits considerable shearing into the moving pile. Note also that the ranges of δ and ϕ stated above cover similar intervals, making inferences from laboratory results to large scale snow avalanches possible, since these are the only two phenomenological parameters in the SH-model with which the material response of a granular avalanche is described.

Data on measured velocity profiles are scarce for both, field and laboratory experiments. Velocity profiles were measured at selected points in artificially released avalanches by Dent et al. [3] for an avalanche in Montana. From a shelter behind a rock nose in the avalanche track the passing avalanche was observed through a window from bottom to top and pure plugflow was observed. Gubler and others [9, 10] used radar Doppler measurements to determine the depth variation of the downhill velocity in an artificially released flow avalanche at the Lukmanier pass in Switzerland; shearing was observed, but it was small, and a statement that it needed to be accounted for was not conclusive. Kern et al. [20] performed chute experiments at Weißfluhjoch, Switzerland, 2680 m a.s.l in a 38 m long rectangular channel with snow and observed that their artificial snow avalanches suffered shearing within the lower most layer, approximately covering 20–30% of the avalanche depth, above which plug flow and below which sliding was observed. Kern et al. roughened the bed artificially so that the bed friction angle may have been large, above say 30°, but they did not provide measured values. So, the experiments likely constitute a situation not typical for flow avalanches.

Eckart et al. [4] conducted laboratory experiments with sand on plexiglass and used Particle Image Velocimetry (PIV) techniques to view the moving mass from above, below and from the side, so measuring the surface and basal velocity as well as its profile at the sidewall of the uniform steady flow. Chutes, 65, 185 and 285 cm long and 27,5 cm wide, inclined at 30°, 35°, 40° and 45° were used. Shearing was observed immediately at the outlet of the material, but disappeared after a distance of 50 cm. Below this region of flow establishment basal and surface velocities were equal with a relative deviation of less than 3.5%. The shearing in the flow establishment region depends on the inclination angle of the chute and the constructive details of the outlet mechanism. In this case the granular material is released from a tank by quickly lifting a gate, thus freeing the particles along a line perpendicular to the base. Because of the basal friction the bottom particles are held back, whilst the top particles are free to move. This automatically introduces a shearing that is weakened as the material moves down the slope as a free-surface flow.

Pudasaini and Hsiau [27] conducted similar experiments with a laboratory chute consisting of an inclined plane that merges via cylindrical segment into a horizontal plane but this time the flow is completely three-dimensional, unconfined, unsteady and non-uniform. PIV measurements were made from above and below in the steep portions of the chute close to the transition region with similar results as reported above: The mean deviation of velocities at the base and the free surface is no more than 3%.

We conclude, *a depth averaged model based on uniform velocity profiles provides most likely an accurate description of the dynamics of flow avalanches on smooth beds.*

2.5 Mohr–Coulomb behaviour

Because in a depth integrated model only the stress states at the free surface and at the base enter the description, a detailed model for the mechanical constitutive behaviour of the stresses is not needed. Nevertheless, the granular structure of the material is still thought to be important insofar as active and passive stress states are distinguished according to whether the flow is extending or compressing in the direction of the stress considered.

The following approximate description of the Mohr–Coulomb behaviour is likely the most critical assumption of the model. It is based on the observation of real flow avalanches that the motion is primarily unidirectional, and transverse shearing is small. Consider a local Cartesian coordinate system at a basal point, in which x is in the downhill direction, y is transverse and z is orthogonal to the two, Fig. 1a. Moreover, consider an infinitesimal cube (its lower face lies in the sliding surface) with the stress vectors as indicated on the visible faces; p_{zz} is the overburden pressure and τ_{xz} the shear traction, at the base as exerted on the sliding surface; p_{yy} is the pressure exerted on faces of the cube normal to the y-direction. It is assumed that the shear stresses τ_{xy} and τ_{yz} are negligibly small, so that p_{yy} is very close to a principal stress, which will be assumed; τ_{xy} is small since transverse shearing is supposed to be small – the motion is practically all downhill – and τ_{yz} cannot be large, because, by construction, x is in the direction of the local velocity. Given the pair (p^b_{zz}, τ^b_{xz}) (b for base), it must lie in the stress plane (p, τ) on the line through the origin, forming the angle δ with the p-axis. All stress states on planes at the base perpendicular to the y-axis then lie on the active (dashed) or passive (solid) circles through (p^b_{zz}, τ^b_{xz}) that are tangent to the wedge with

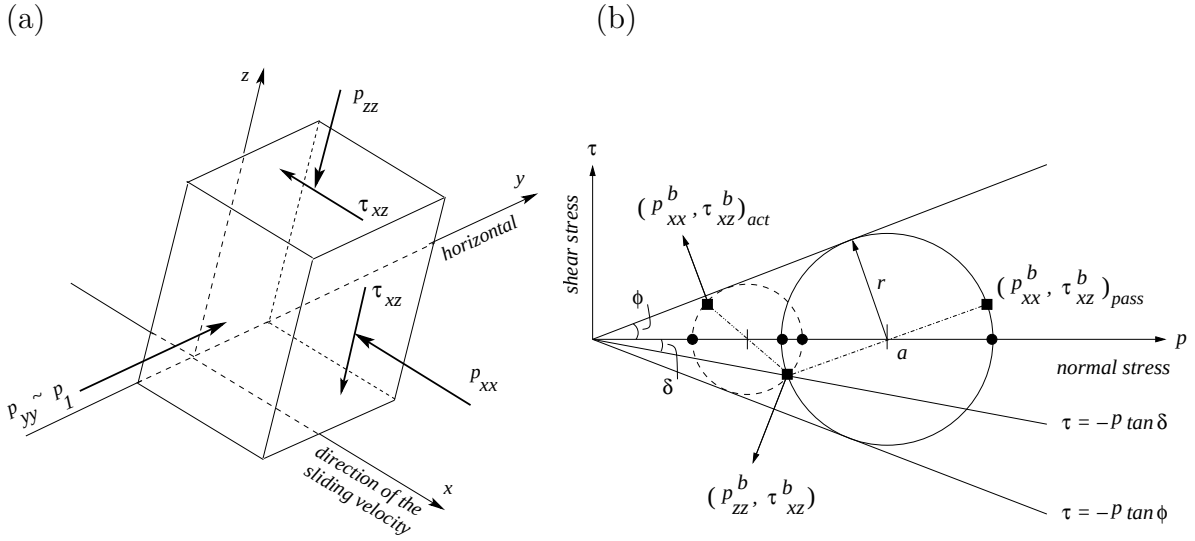

Figure 1: (a) Volume element at the base of an avalanche. The local coordinates x, y and z are in the direction of the sliding velocity, perpendicular to it and tangential to the bed and normal to the two directions. The stress vectors indicated on the front and top faces are those components which are significant for the Mohr circle argument. The omitted components are small. (b) Mohr stress plane (in which pressure is positive). The point representing the traction on the sliding surface lies on the straight line forming the angle δ with the p-axis. Through this point an active and a passive Mohr circles can be drawn which touch the wedge with opening angle 2ϕ On these circles lie the stress states $(p^b_{xx}, \tau^b_{xz})_{\mathrm{act/pass}}$ as well as the principal stresses indicated by $\bullet$.

vertex angle 2δ, and the points $(p^b_{xx}, \tau^b_{xz})_{\mathrm{act,pass}}$ are obtained by a rotation of 180° on these circles. Of the two possibilities "act" ("pass") is selected if the normal strain rate in the x-direction, $\partial u/\partial x$ is positive, i.e., extensional (negative, i.e., compacting). The principal stresses and the direction of the elements at which they apply can also be calculated; they are given as indicated by the solid circles in the Mohr diagram in Fig. 1b. Given (p^b_{zz}, τ^b_{xz}), all stress states can be expressed in terms of these as well as ϕ and δ.

There remains the determination of p^b_{yy}. To this end it will now be assumed that of the three principal stresses two will agree with one another. This ad-hoc assumption makes the determination of p^b_{yy} unique and sets it equal to one of the four principal stresses on the two circles shown in Fig. 1b. The sign of the longitudinal normal strain rate, $\partial u/\partial x$, selects the active or passive circle, and the sign of the transversal normal strain rate, $\partial v/\partial y$, will determine the smaller ($\partial v/\partial y > 0$) or the larger ($\partial v/\partial y < 0$) of the two values on the respective circle. Thus,

$$\frac{p^b_{xx}}{p^b_{zz}} = K_{x_{\mathrm{act/pass}}}(\phi, \delta), \quad \frac{p^b_{yy}}{p^b_{zz}} = K^{y_{\mathrm{act/pass}}}_{x_{\mathrm{act/pass}}}(\phi, \delta), \tag{1}$$

where $K_{x_{\mathrm{act/pass}}}$, $K^{y_{\mathrm{act/pass}}}_{x_{\mathrm{act/pass}}}$ are the earth pressure coefficients that are functions of ϕ and δ. This is the least rational assumption of all, and it is only justified by the results it produces. It should, however, also be mentioned that the above ad-hoc assumption destroys the rational invariance of the equations about the z-direction perpendicular to

the tangential plane of the reference surface. The reason for this lies in the omission of the stresses τ_{yz} and the preference of the x-velocities in the above construction of (1). Iverson and others [17, 18] in their models do not use it.

At the free surface all stress components must be zero in a cohesionless Mohr–Coulomb material if the traction from above is set to zero. Moreover, since p_{zz} and τ_{xz} are linearly distributed, it is also reasonable to assume a linear dependence for p_{xx} and p_{yy}, connecting (p^b_{xx}, p^b_{yy}) at the base with $(0, 0)$ at the free surface.

3 Performance of the model

3.1 Governing equations [28]

The SH-equations were derived in various different coordinate systems. In appropriately chosen orthogonal curvilinear coordinates they take the following conservative form:

Mass Balance

$$\frac{\partial h}{\partial t} + \frac{\partial}{\partial x}(hu) + \frac{\partial}{\partial y}(hv) = 0, \tag{2}$$

Momentum Balances

$$\begin{aligned} \frac{\partial}{\partial t}(hu) + \frac{\partial}{\partial x}(hu^2) + \frac{\partial}{\partial y}(huv) &= hs_x - \frac{\partial}{\partial x}\left(\frac{\beta_x h^2}{2}\right), \\ \frac{\partial}{\partial t}(hv) + \frac{\partial}{\partial x}(huv) + \frac{\partial}{\partial y}(hv^2) &= hs_y - \frac{\partial}{\partial y}\left(\frac{\beta_y h^2}{2}\right), \end{aligned} \tag{3}$$

$$\begin{aligned} &\beta_x := -\varepsilon g_z K_x, \qquad \beta_y := -\varepsilon g_z K_y, \\ &s_x := g_x - \frac{u}{|\boldsymbol{u}|}\tan\delta\left(-g_z + \lambda\kappa\eta u^2\right) + \varepsilon g_z \frac{\partial b}{\partial x}, \\ &s_y := g_y - \frac{v}{|\boldsymbol{u}|}\tan\delta\left(-g_z + \lambda\kappa\eta u^2\right) + \varepsilon g_z \frac{\partial b}{\partial y}, \\ &\eta := \cos\left(\psi(y) + \varphi(x) + \varphi_0\right), \end{aligned} \tag{4}$$

in which

$$\begin{aligned} K_x = K_{x_{\text{act/pass}}} &= 2\sec^2\phi\left(1 \mp \left(1 - \cos^2\phi/\cos^2\delta\right)^{1/2}\right) - 1, \quad \left(\frac{\partial u}{\partial x} \gtrless 0\right), \\ K_y = K^{y_{\text{act/pass}}}_{x_{\text{act/pass}}} &= \frac{1}{2}\left(K_x + 1 \mp \left((K_x - 1)^2 + 4\tan^2\delta\right)^{1/2}\right), \quad \left(\frac{\partial v}{\partial y} \gtrless 0\right). \end{aligned} \tag{5}$$

Here, x, y are curvilinear coordinates in the directions along and perpendicular to the curved and twisted master curve; h, hu, hv are the avalanche depth and the specific momenta in the x- and y-directions, respectively; g_x, g_y, g_z define the gravity components in the three orthogonal directions x, y, z; $\lambda\kappa$ is the local radius of curvature of the master curve and β_x, β_y define normal pressures in the x- and y-directions, respectively. Moreover, $b(x, y)$ defines the basal surface, i.e., the deviation of the basal topography from the reference surface $z = 0$, whilst φ gives the accumulation of the torsion of the

master curve from an initial position and ϕ_0 is an arbitrary constant, see Pudasaini & Hutter [28]. Equations (2)–(5) form a hyperbolic system of partial differential equations with coefficients which may have jump discontinuities and can be written in standard mathematical form. For their solution the input quantities are the topography ($b(x, y)$, master curve) the internal and bed friction angles, ϕ, δ, and the initial values for h, u, v; the output is defined by the three conservative functions $h(x, y, t)$, $hu(x, y, t)$ and $hv(x, y, t)$ or equivalently $h(x, y, t)$, $u(x, y, t)$ and $v(x, y, t)$.

3.2 Numerical schemes

In order to test the above model equations against avalanche events either in Nature or in the laboratory, a numerical integration scheme must be constructed. Early attempts [5, 7, 8, 12, 13, 14, 21, 34, 35, 45] used Lagrangian finite difference schemes with central difference approximation and leap frog temporal integration steps. These approaches made addition of explicit numerical diffusion necessary, but it was held minimal and made operative where gradients of the avalanche thickness and velocities became large. These methods were not able to capture shocks and may have smoothed these out. Shock capturing finite difference techniques were introduced later. Tai [38] and Tai et al. [39] used them in a two-dimensional Eulerian shock capturing scheme and a one-dimensional front-tracking method, respectively. Wang et al. [44] employed a high resolution approach, namely the non-oscillatory central (NOC) scheme, and compared different cell reconstruction techniques – four second-order total variation diminishing (TVD) limiters and a three-order essentially non-oscillatory (ENO) cell reconstruction scheme. Of the numerical methods under consideration the NOC scheme with the Minmod TVD limiter showed the best performance in chute flows down a parabolic channel merging into a horizontal plane. These Eulerian schemes, whereas superior to the above mentioned central difference schemes, are comparably accurate to other shock capturing methods. Koschdon and Schaefer [22] use an arbitrary Lagrangian-Eulerian finite-volume method, where unstructured boundary-fitted moving grids are employed to follow the free boundary. The underlying flow solver consists of a Godunov-type approach in the space-time domain, and the fluxes are calculated using Riemann solvers. Vollmöller [43], on the other hand, uses a wave propagation method in the context of unstructured finite volumes and on the basis of Godunov-type schemes with spatially discretized flux functions.

Comparisons of numerical solutions with laboratory chute flows have been conducted in [5, 7, 8, 11, 13, 14, 21, 35, 38, 39, 40, 41, 45] and will not be repeated here. However, the results of the motion of a finite mass of sand down a plane plexiglass chute merging into a horizontal runout are summarised in Fig. 2. It compares the geometry of the deposit as obtained experimentally and computationally by Pudasaini [27] using the integration technique in Wang et al [44] and Tai [38]. The details are given in the figure caption.

The true test of a shock capturing integration method is a situation where abrupt changes of flow heights and/or velocities occur. Experiments were conducted in the Darmstadt laboratory[3] for uniform granular flows down an inclined plane that is diverted by a pyramid, a circular cylinder or a wall. Shock waves, dead zones and/or particle free

[3]Laboratory of the Department of Mechanics, Darmstadt University of Technology, Darmstadt, Germany.

a) Final deposit of a granular avalanche obtained by the theory

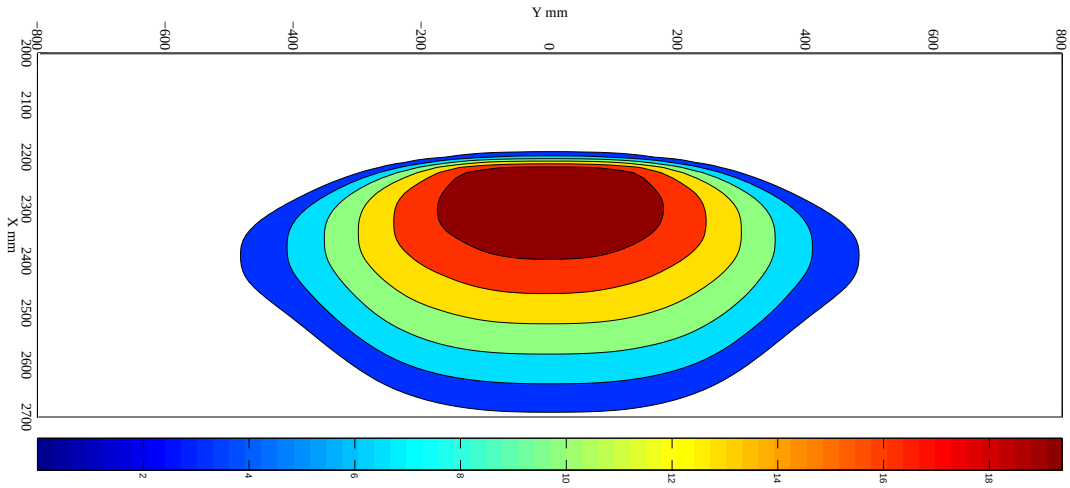

b) Final deposit of a granular avalanche obtained by the experiment

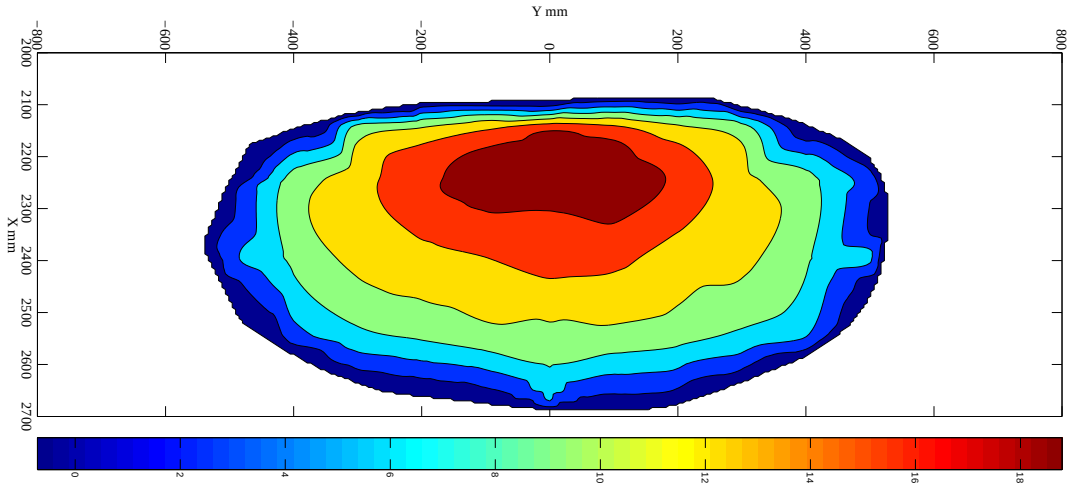

Figure 2: Final deposit of a granular avalanche moving down a plexiglass plane with 45° inclination angle merging into a horizontal plane. The panels show height level lines of the deposit at rest as obtained by the theory (above) and experiment (below) and as determined by Pudasaini, [27], using the integration method described in Wang et al [44].

regions were formed that were computationally reproduced by Gray et al. [6] using the NOC scheme introduced by Nessyahu & Tadmor [25] and extended to multidimensions by Jiang & Tadmor [19] and Lie & Noelle [23]. The results of Gray et al. can also be reproduced by using the integration routine of Wang et al. [44].

A robust test of an integration code for the SH-equations is the flow of a finite granular mass down an inclined plane impinging on obstructions, partly circumflowing and partly overflowing these, and then merging into a horizontal plane. The topography of the deposited mass depends strongly on the flow around and over the obstruction. For a high wall perpendicular to and across the inclined plane, which only allows flow around the sides of the wall, the deposited mass, computed with the NOC scheme and

(a) granular flow of a finite mass past a wall

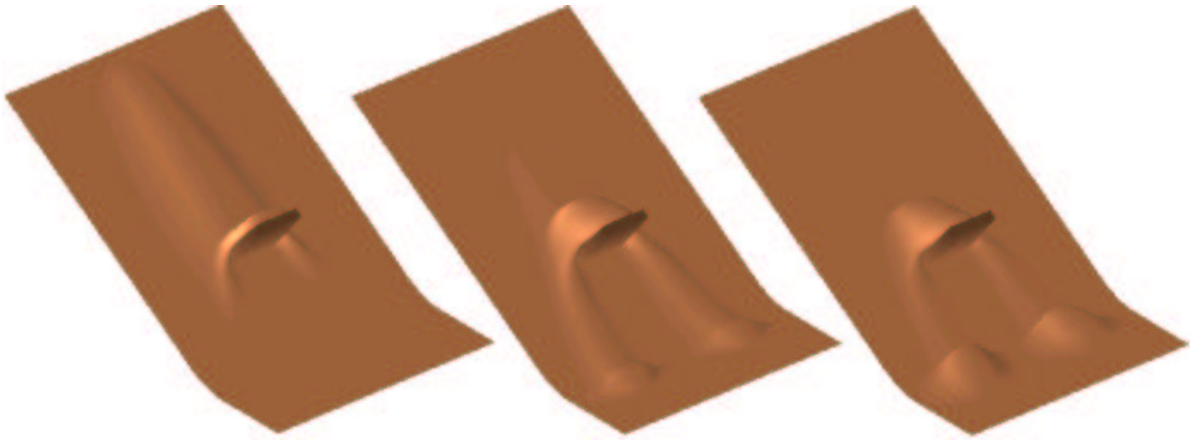

$t = 7$ $t = 14$ $t = 21$

(b) granular flow of a finite mass past a tetrahedral wedge

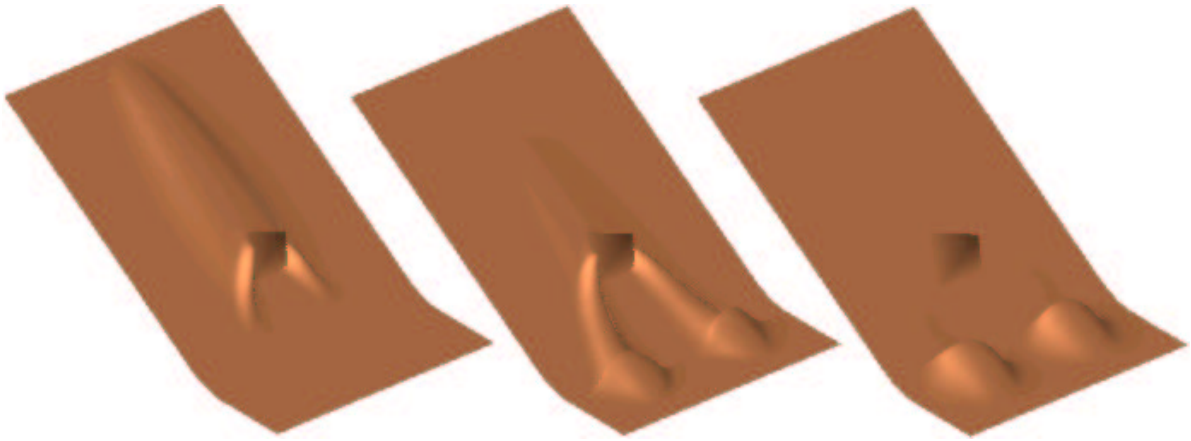

$t = 7$ $t = 14$ $t = 21$

Figure 3: Three-dimensional geometries of a granular flow down an inclined (by 40°) plane and into the horizontal plane past a wall (above) and a tetrahedral wedge (below) both having a maximum dimensionless height of $H = 5$ for three different dimensionless times $t = 7, 14, 21$.

the Minmod limiter described in Wang et al. [44] consists of two separate heaps with lobes connected to the sides of the wall at much higher elevation, which are unrealistic and not reproduced when the integration is performed for the flow over and around a tetrahedral wedge. Admittedly, when impinging a wall, the SH-equations can not be a valid set of equations to properly predict the flow in the immediate vicinity of the wall. The formation of the dead zone behind the wall, however, changes the geometry of the flow in the right direction. In any case, a numerical scheme that does not show these lobes would certainly be more trustworthy; inspite of this, corroboration of the solution by experiment is still necessary. Fig. 3 shows some deposited masses for this case and the figure caption explains details.

It is apparent that numerical integration of the strongly convective SH-equations requires a robust numerical programme which must be tested in benchmark problems

involving shocks, dead zones and granular free regions. Of course, less sophisticated discretisations may prove adequate when shocks or steep gradients of the fields do not arise. In any case, only a trustworthy numerical programme can be used when computational results are compared with experiments.

3.3 Comparison with observations

It is not necessary here to repeat the many comparisons that were conducted with numerical output and experimental findings. In the laboratory the moving granular masses were photographed with fast speed cameras operating between 4 and 15 frames per second. This simple technique allowed comparison of the avalanche circumference as the moving mass evolved through time from initiation to runout. With less accuracy the photos also permitted estimation of the velocity distribution. However, the latter became only experimentally available, once the particle image velocimetry technique was introduced. Excellent comparisons were obtained in confined flows down chutes consisting of plane segments [14], an exponentially [13] or concave-convexly [7] curved profile in which a single hump was split into two separate depositions above and below the topographic bump. Further comparisons were performed for transversely unconfined flows down an inclined plane merging into a horizontal plane [8, 21, 43], or a parabolic channel merging into a horizontal plane with curved thalweg [5, 45]. Steep shock-like depth changes arose in the transition zones from supercritical (dilating) to subcritical (compacting) flow conditions that could well be reproduced by the shock-capturing integration techniques, but shock forming flows down inclined planes, diverted by wedges, walls and cylinders [40] could only adequately be reproduced by the shock capturing techniques [6, 44]. While these results are pleasing and provide support for the SH model, there still is the need for comparison of experiments and theory when dead zones are formed. Such studies are presently under way.

Whereas laboratory experiments can be studied under isolated, well controlled conditions, this is not so for natural avalanche events, even if these are artificially released. Comparison of the SH-equations with such events are very rare and generally less convincing than for granular avalanches in the laboratory. Problems arise with the estimation of δ and ϕ, the discretisation of the topography, the estimation of the moving mass, the neglection of entraining mass from below and possible deposition, which may be present, in some instances to a large extent. The only example we know is reported in [46, 47].

In this regard it seems important that input parameters of the SH-model are randomly varied within practically reasonable ranges and that probability distributions are determined for the output quantities.

In summary, it appears that computational routines are now available which reliably allow construction of trustworthy solutions of the SH-equations. The computational output, when compared with laboratory experiments proved the equations to be a reliable model for most tested configurations. Further scrutiny does, however, seem to be necessary for geometrically more complex situations for which the validity of the model seems to be limited. Predictions or post-computations of real avalanches should always be performed with a statistical input such that input parameters are varied in their ranges of expectation and probability distributions are determined for the output quantities.

4 Outlook

This brief review of the depth integrated SH-equations allows the following inferences to be drawn:

- For laboratory avalanches starting on steep slopes the model seems to reproduce the motion of a finite mass of granular material down inclines from initiation to runout pretty well including shock capturing features. Additional studies are necessary for those cases in which obstructions are hit in the vicinity of which the shallowness assumption is formally violated.

- Comparison of the model equations with field events – either snow or rock avalanches – are scarce and insufficiently conclusive. Post-calculations of the Madlein avalanche in Austria seems to indicate that the Coulomb basal friction law is insufficient and requires complementation by a viscous contribution.

- The model equations have not yet been tested for stresses exerted on walls of obstructing objects. Are computed wall pressures and shear tractions representative for the corresponding tractions in the experiment? Practically, these quantities are important ones, and suitability of the model equations for these would make the model much more valuable.

- There is a need for a wider application of the model to situations with natural topographies. Such topographies should also be reproduced in physical models at smaller scale to test the robustness of the equations as well as the reproducibility of avalanche motion performed with these.

- Avalanches starting from gentle slopes of inclination angles $\leq 30^\circ$ and on bumpy beds behave differently, and they often come to a premature stop. They generally are less dangerous.

Finally, it ought to be mentioned that this review and all the work reported herein does not touch the practically significant entrainment mechanism from the ground. If snow avalanches move over a layer of deposited snow, they often entrain snow from this layer and grow in mass. This often happens and significantly influences the dynamics of an avalanche. To my knowledge, there is only one paper attacking this problem [37]. Of course, in real avalanche events the measurement of the entrained mass is difficult and in most situations not controllable. Needless to say, that this adds further to the uncertainty in comparisons of real avalanche events with computational output of any model.

Acknowledgements

This work was done while the first author was at the Isaac Newton Institute of the University of Cambridge as a member of the programme: “Granular and particle laden flow”. Financial support is gratefully acknowledged.

References

[1] Ancey, C. (2001) Snow Avalanches. In: Balmforth, N.L. Provenzale, A. (Eds.) Lecture Notes in Physics, LNP Vol. 582: Geomorphological Fluid Mechanics, Springer, 319-338

[2] Ancey, C., C. Meunier, (2003) Estimating bulk rheological properties of flowing snow avalanches from field data, Journal of Geophysical Research (in print)

[3] Deut, J. D., K. J. Burrell, D. S. Schmidt, M. Y. Louge, E. E. Adams and T. G. Jazbutis (1998) Density, velocity and friction measurements in a dry snow avalanche. Annals of Glaciol. 26, 247-252

[4] Eckart, W., J.M.N.T. Gray and K. Hutter (2003) Particle Image Velocimetry (PIV) for granular avalanches on inclined planes. In: Dynamic Response of Granular and Porous Materials under Large and Catastrophic Deformations, edited by K. Hutter and N. Kirchner, Lecture Notes in Applied and Computational Mechanics 11 (Springer, Berlin, 2003) pp 195-218

[5] Gray, J.M.N.T., M. Wieland and K. Hutter, Gravity driven free surface flow of granular avalanches over complex basal topography, Proc. R. Soc. London A 455, 1841-1874 (1999)

[6] Gray, J.M.N.T., Y.-C. Tai and S. Noelle. Shock waves, dead zones and particle free regions in rapid granular free surface flows. J. Fluid Mech. 491, pp 160-181

[7] Greve, R. and K. Hutter, The motion of a granular avalanche in a convex and concave curved chute: Experiments and theoretical predictions, Phil. Trans. R. Soc. London A 342, 573-604 (1993)

[8] Greve, R., T. Koch and K. Hutter, Unconfined flow of granular avalanches along a partly curved surface. Part I: Theory, Proc. R. Soc. London A 445, 399-413 (1994)

[9] Gubler, H., M. Hiller, G. Klausegger and U. Suter, Messungen an Fließlawinen, Report 41, Eidgenössisches Institut für Schnee- und Lawinenforschung, Davos (1986)

[10] Gubler, H. Dense-flow avalanches, a discussion of experimental results and basic processes. In: International Workshop on rapid gravitational mass movements, edited by L. Buisson and G. Grugnot, pp. 126-127, Cemagref, Grenoble (1993)

[11] Hutter, K. Avalance dynamics. In: Hydrology of disasters, edited by V.P. Singh, (Kluwer Academic Publ., Dordrecht, Boston, London, (1996) pp. 317- 394

[12] Hutter, K. and R. Greve, Two-dimensional similarity solutions for finite-mass granular avalanches with Coulomb- and viscous-type frictional resistance. J. Glac. 39, 357-372 (1993)

[13] Hutter, K. and T. Koch, Motion of a granular avalanche in an exponentially curved chute: experiments and theoretical predictions, Phil. Trans. R. Soc. London, A 334, 93-138 (1991)

[14] Hutter, K., T. Koch, C. Plüss and S. B. Savage, The dynamics of avalanches of granular materials from initiation to runout. Acta Mech. 109, 127-165 (1995)

[15] Hutter, K. and Y. Nohguchi, Similarity solutions for a Voellmy model of snow avalanches with finite mass, Acta Mech. 82, 99-127 (1990)

[16] Hutter, K. M. Siegel, S.B. Savage and Y. Nohguchi, Two dimensional spreading of a granular avalanche down an inclined plane, Part I. Theory, Acta Mechanica 100, 37-68 (1993)

[17] Iverson, R. M., The physics of debris flows, Rev. Geophys., 35, 245-296, (1997)

[18] Iverson, R. M., and R. P. Denlinger, Flow of variably fluidized granular masses across three-dimensional terrain. 1. Coulomb mixture theory, J. Geophys. Res. B, 106, 537-552, (2001)

[19] Jiang, G. and E. Tadmor, Non-oscillatory central schemes for multidimensional hyperbolic conservation laws. SIAM J. Sci. Comput. 19, 1892-1917, 1997

[20] Kern, M. A., F. Tiefenbacher and J. N. McElwaine (2003) Energy balance in chute flows of snow. Cold Reg. Sci. Tech. (in press)

[21] Koch, T., R. Greve and K. Hutter, Unconfined flow of granular avalanches along a partly curved chute. II. Experiments and numerical computations, Proc. Roy. Soc. London A 445, 415-435 (1994)

[22] Koschdon, K. and M. Schäfer, A Lagrangian-Eulerian finite-volume method for simulating free surface flows of granular avalanches. In: Dynamic Response of Granular and Porous Materials under Large and Catastrophic Deformation, edited by K. Hutter and N. Kirchner, Lecture Notes in Applied and Computational Mechanics 11 (Springer, Berlin, 2003) pp. 83-108

[23] Lie, K.A. and S. Noelle (2003) An improved quadrature rule for the flux-computation in staggered central difference schemes in multidimensions. J. Sci. Computing. 18, pp 69-80

[24] McClung, D.M. and Schaerer, P. A., The Avalanche Handbook, The Mountaineers, Seattle, (1993)

[25] Nessyahu, H. and E. Tadmor, Non-oscillatory central differencing for hyperbolic conservation laws, J. Compt. Phys. 87, 408-463 (1990)

[26] Perla, R., T.T. Cheng and D. M. McClung, A two-parameter model of snow-avalanche motion, J. Glaciol., 26, 197-202 (1980)

[27] Pudasaini, S.P, Dynamics of Flow Avalanches over Curved and Twisted Channels: Theory, Numerics and Experimental Validation. Ph. D. Thesis, Darmstadt University of Technology, Dramstadt, Germany (2003)

[28] Pudasaini, S.P. and K. Hutter, Rapid shear flows of dry granular masses down curved and twisted channels, J. Fluid Mech., 495, 193-208 (2003)

[29] Pudasaini, S.P., W. Eckart and K. Hutter, Gravity driven rapid shear flows of dry granular masses in helically curved and twisted channels, Math. Models Meth. Appl. Sci., 13 (7), 1019-1052 (2003)

[30] Pudasaini, S.P., K. Hutter and W. Eckart, Gravity-driven rapid shear flows of dry granular masses in topographies with orthogonal and non-orthogonal metrics. In: Dynamic Response of Granular and Porous Materials under Large and Catastrophic Deformation, edited by K. Hutter and N. Kirchner, Lecture Notes in Applied and Computational Mechanics 11 (Springer, Berlin, 2003) pp. 43-82.

[31] Salm, B. (1966) Contribution to avalanche dynamics. IAHS AISH Publ. 69. 199-214

[32] Salm, B., H. Gubler, Measurement and Analysis of dense flow of avalanches. Annals of Glaciol. 6, 26-34 (1985)

[33] Savage, S.B. and Y. Nohguchi, Similarity Solutions for Avalanches of Granular Materials Down Curved Beds. Acta Mechanika, 75, 153-174 (1988)

[34] Savage, S.B. and K. Hutter, The motion of a finite mass of granular material down a rough incline, J. Fluid Mech. 199, 177-215 (1989)

[35] Savage, S.B. and K. Hutter, The dynamics of avalanches of granular materials from initiation to runout. Part I: Analysis, Acta Mechanica 86, 201-223 (1991)

[36] Schaerer, P.A., Friction coefficients and speed of flowing avalanches, in Symposium Mécanique de la Neige, edited by the International Association of Hydrological Sciences, pp. 425-432 (1974)

[37] Sovilla, B., F. Sommavilla, A. Tomaselli, Measurements of mass balance in dense avalanche events, Ann. Glaciol., 32, 230-236, (2001)

[38] Tai, Y.C., Dynamics of Granular Avalanches and their Simulations with Shock-Capturing and Front-Tracking Numerical Schemes. Ph. D. thesis, Darmstadt University of Technology, Darmstadt 2000

[39] Tai, Y.C., S. Noelle, J.M.N.T. Gray and K. Hutter, Shock-capturing and front-tracking methods for granular avalanches, J. Comput. Phys. 175, 269-301 (2002)

[40] Tai, Y.C., Y. Wang, J.M.N.T. Gray and K. Hutter, Methods of similitude ind granular avalanche flows. In: Advances in Cold-Regions Thermal Engineering and Sciences, edited by K. Hutter, Y. Wang and H. Beer, Lecture Notes in Physics 533 (Springer, Berlin, 1999) pp. 415-428

[41] Tai, Y.-C., J.M.N.T. Gray and K. Hutter (2001) Dense Granular Avalanches: Mathematical Description and Experimental Validation. In: Balmforth, N.L., Provenzale, A. (Eds.) Lecture Notes in Physics, LNP Vol. 582: Geomorphological Fluid Mechanics. Springer, 339-366

[42] Voellmy, A. (1955) Über die Zerstörungskraft von Lawinen. Schweizerische Bauzeitung 73, 159-162, 212-217, 246-249, 280-285

[43] Vollmöller, P. (2003) A shock-capturing wave propagation method for dry and saturated granular flows. J. Comp. Physics (submitted)

[44] Wang, Y., K. Hutter and S.P. Pudasaini (2003) The Savage-Hutter theory: a system of partial diffential equations for avalanche flows of snow, debris and mud. ZAMM (in press)

[45] Wieland, M. J.M.N.T. Gray and K. Hutter, Channelized free surface flow of cohesionless granular avalanche in a chute with shallow lateral curvature, J. Fluid Mech. 293, 73-100 (1999)

[46] Zwinger, T., Dynamik einer Trockenschneelawine auf beliebig geformten Berghängen. Ph. D. thesis, Vienna University of Technology, Vienna 2000

[47] Zwinger, T., A. Kluwick and P. Sampl, Numerical simulation of dry-snow avalanche flow over natural terrain. In: Dynamic Response of Granular and Porous Materials under Large and Catastrophic Deformation, edited by K. Hutter and N. Kirchner, Lecture Notes in Applied and Computational Mechanics 11 (Springer, Berlin, 2003) pp. 161-194